ADVANCED MATERIALS
www.advmat.de

Reduction of 5-Hydroxymethylfurfural to 2,5-Bis(hydroxymethyl)Furan at High Current Density using a Ga-Doped AgCu:Cationomer Hybrid Electrocatalyst

Cong Tian, Jiaqi Yu, Daojin Zhou, Huajie Ze, Hengzhou Liu, Yuanjun Chen, Rong Xia, Pengfei Ou, Weiyan Ni, Ke Xie, and Edward H. Sargent**

Hydrogenation of biomass-derived chemicals is of interest for the production of biofuels and valorized chemicals. Thermochemical processes for biomass reduction typically employ hydrogen as the reductant at elevated temperatures and pressures. Here, the authors investigate the direct electrified reduction of 5-hydroxymethylfurfural (HMF) to a precursor to bio-polymers, 2,5-bis(hydroxymethyl)furan (BHMF). Noting a limited current density in prior reports of this transformation, a hybrid catalyst consisting of ternary metal nanodendrites mixed with a cationic ionomer, the latter purposed to increase local pH and facilitate surface proton diffusion, is investigated. This approach, when implemented using Ga-doped Ag-Cu electrocatalysts designed for *p–d* orbital hybridization, steered selectivity to BHMF, achieving a faradaic efficiency (FE) of 58% at 100 mA cm^{-2} and a production rate of 1 mmol cm^{-2} h^{-1}, the latter a doubling in rate compared to the best prior reports.

1. Introduction

Biomass, which incorporates CO_2 captured from air and soil, is a candidate feedstock to reduce the carbon intensity (CI) of fuels and chemicals. Since its transport to centralized processing plants adds cost and CI,[1] it is of interest to explore modular, onsite, biomass refining, of the type that electrochemical transformations can potentially provide.[2]

C. Tian, J. Yu, D. Zhou, H. Ze, H. Liu, Y. Chen, R. Xia, P. Ou, W. Ni, K. Xie, E. H. Sargent
Department of Chemistry
Northwestern University
2145 Sheridan Rd, Evanston, IL 60208, USA
E-mail: ke-xie@northwestern.edu; ted.sargent@northwestern.edu
E. H. Sargent
Department of Electrical and Computer Engineering
Northwestern University
2145 Sheridan Rd, Evanston, IL 60208, USA

The ORCID identification number(s) for the author(s) of this article can be found under https://doi.org/10.1002/adma.202312778

DOI: 10.1002/adma.202312778

5-Hydroxymethylfurfural (HMF) is a biomass intermediate obtained from the dehydration of cellulosic feedstocks,[3] and is a top-10 biobased platform chemical.[4] The multiple functional groups and the furan ring of HMF enable versatile upgrade pathways, both oxidatively and reductively. In recent years, electrocatalysis has emerged as a powerful tool to convert HMF into valuable chemicals in light of its mild reaction conditions, its replacement of oxidant/reductants, and its potential to decrease carbon intensity when it is powered using renewable electricity.[5]

On the reductive side, electrocatalytic hydrogenation (ECH)[1] utilizes water directly as a hydrogen source at ambient temperatures and pressures, with the goal of producing high-energy-density fuels and valorized chemicals. Among electro-valorized HMF products, 2,5-bis(hydroxymethyl) furan (BHMF)[6] – a biopolymer precursor in the production of bio-derived polyesters (**Figure 1A**) – has been found to exhibit excellent selectivity via ECH.[7]

Unfortunately, prior reports of HMF to BHMF have been limited to batch processes (e.g., in H-cells), and reported current densities have so far remained below 50 mA cm^{-2}.[8] Operating at low intensities was necessary to minimize the competing hydrogen evolution reaction (HER) in aqueous electrolyte. Li and colleagues[7b] developed a flow system (membrane electrode assembly, MEA) that coupled HMF oxidation to 2,5-furandicarboxylic acid (FDCA) and HMF reduction to BHMF in one electrolyzer. A high BHMF faradaic efficiency (FE) of ≈80% was achieved at 2 mA cm^{-2} using a 50 mM HMF solution at pH 9; when the current density was increased to industrially relevant current densities, the FE to BHMF went down to 24%, with the competing HER becoming the dominant reaction.

We posited that the joint design of the catalyst, integrated with an ionomer, could potentially increase selectivity to BHMF, and work against the competing HER at high current densities. Doping using *p*-block metals has been identified as a means to modify catalyst structure in electrochemistry.[9] *p–d* orbital hybridization introduced by *p*-block metal doping stabilizes active sites and enhances intermediate binding strength under electrochemical conditions.[9a] This in turn promotes selectivity in electrocatalytic production. We pursued *p–d* orbital hybridization introduced by

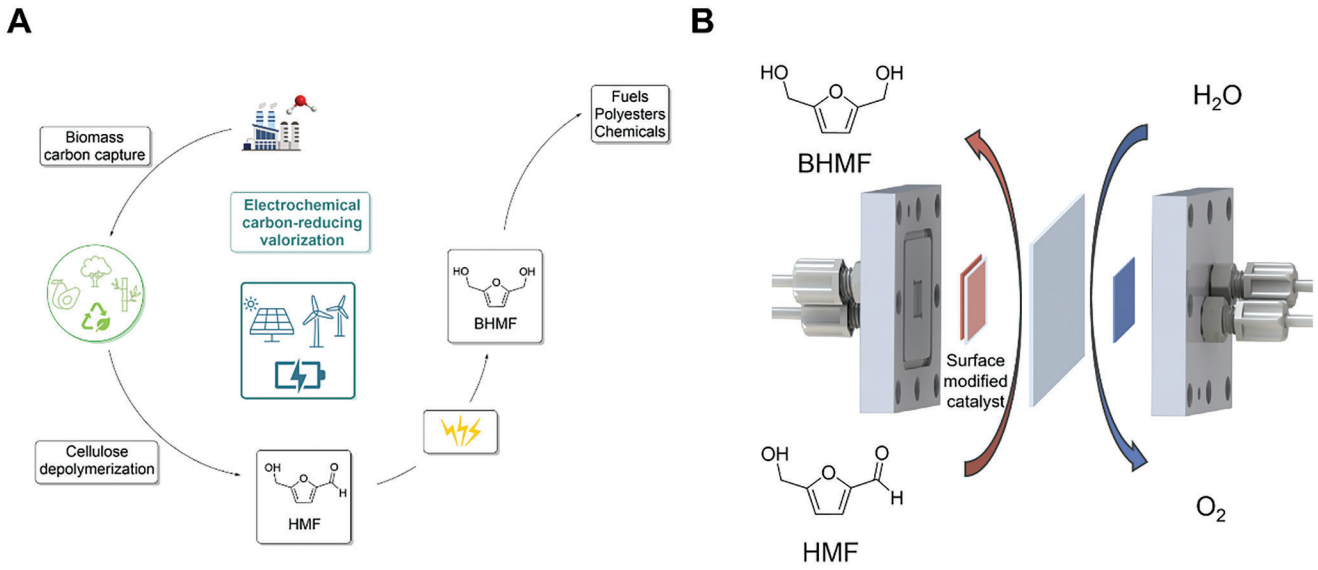

Figure 1. Electrocatalytic hydrogenation of HMF to BHMF. A) Schematic illustrating electrochemical biomass valorization for BHMF production. B) Selective HMF electrochemical reduction to BHMF in an MEA system.

p-block Ga-doped Ag-Cu nanodendrite electrocatalysts, our concept to offer active sites for selective HMF reduction to BHMF while suppressing the competing HER.

We further considered augmenting the electrocatalyst using ionomers, an approach that has shown potential in manipulating the local environment and, consequently, selectivity to products.[10] Notably, using cationic ionomers in cathodic reduction reactions has shown promise in advancing electrocatalysis toward higher current densities.[11] We incorporated a cationic ionomer layer[10a,11] onto the catalyst surface to modify the cathodic local pH to a suitable alkaline value, promoting hydrogen atom transfer (HAT) on the catalyst to favor BHMF formation.

2. Results and Discussion

2.1. Synthesis and Characterization of ECH Catalysts

We began by screening ECH catalysts (Table S1, Supporting Information) and operating conditions (Table S2, Supporting Information) to evaluate selectivity to BHMF in HMF reduction in a continuous-flow MEA electrolyzer. Several candidate transition metal nanoparticles with similar morphology were introduced in the electrolyzer and tested as the cathode in HMF reduction. BHMF was detected in the catholyte using ^{1}H NMR (Figure S1, Supporting Information). Previous reports[6b,c,12] indicated enhanced utilization of hydrogen species on the AgCu surface at low current densities, making it a suitable catalyst for selective HMF reduction. Similarly, AgCu showed a BHMF FE of 44% at 100 mA cm^{-2}. We also observed, in ^{1}H NMR, the formation of the by-product, 5,5′-bis(hydroxymethyl)hydrofuroin (BHH), attributable to HMF dimerization.[13]

We then sought to tune further the electronic structure of the Ag-Cu nanoalloy electrocatalyst. We synthesized a set of ternary catalysts X-doped Ag-Cu (X = Ir, Rh, Pt) using a modified two-step galvanic replacement method,[14] loaded these nanoparticles onto hydrophilic carbon paper, and characterized their performance in HMF ECH. In the case of Ga-doped Ag-Cu, Ga is introduced via surface etching and ion exchange.

Ga-doped Ag-Cu nanoparticles showed a dendritic structure (scanning transmission electron microscopy, STEM, **Figure** 2A,B). Atomic resolution STEM (AR-STEM) and fast Fourier transform (FFT) diffraction indicate that the branches of the dendrites exhibit an fcc crystal structure, consistent with Ag and Cu crystal structures (Figure 2C). Powder X-ray diffraction (XRD) indicates Cu-Ag bimetal (Figure S2, Supporting Information). Scanning electron microscopy-energy dispersive X-ray spectroscopy (SEM-EDS) showed, within its spatial resolution of 10 μm, a uniform distribution of Ga, Ag, and Cu as Ga-doped Ag-Cu (Figure 2D and Table S3, Supporting Information). We applied X-ray photoelectron spectroscopy (XPS) (Figure S3, Supporting Information) to Ga-doped Ag-Cu and confirmed the incorporation of Ga into the AgCu catalyst, which aligns well with the EDS result.

We then explored ionomer layer coating strategies to control the surface species and electrode local pH. We implemented cation ionomer modification by deploying a layer of Nafion, following a procedure outlined in a previous report.[10a] From SEM-EDS mapping for F and S (Figure 2E), we found a substantially uniform coating of sulfonic-functionalized fluoropolymer consistent with the formation of PFSA-coated metal catalysts.

2.2. Incorporation into a Membrane Electrode Assembly System

In light of the initial results (Table S2, Supporting Information), we carried out electrolysis in 1 M $NaHCO_3$. From Ga-doped Ag-Cu we reached 51% FE at 100 mA cm^{-2} with a full cell voltage of 3.12 V (**Figure** 3A).

When we employed a catalyst that included a thin layer of the cationic ionomer atop Ga-doped Ag-Cu, BHMF FE increased to

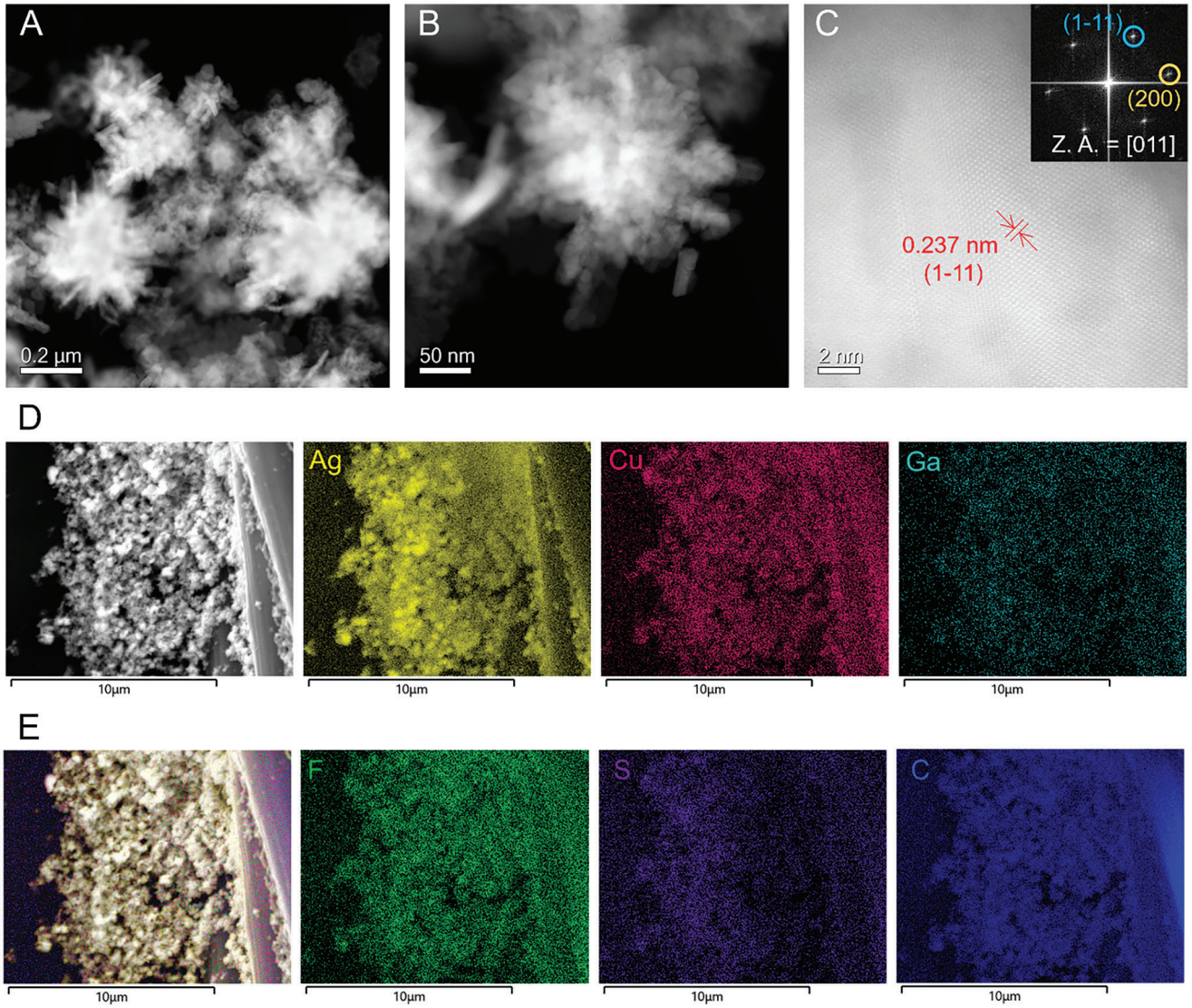

Figure 2. Structural and compositional characterization of ECH catalyst for HMF reduction. A,B) STEM images of Ga-doped Ag-Cu nanomaterials showing dendritic structure. C) AR-STEM image of Ga-doped Ag-Cu; inset: FFT of (C). Lattice fridge shown in (C) aligns with the fcc crystal structure viewing from [011] zone axis (ZA). D,E) SEM and EDS elemental mapping of Ga-doped Ag-Cu electrode: yellow: Ag; red: Cu; Cyan: Ga; green: G; purple: S; and blue: C.

58% (Figure 3B,C). The cation exchange capacity of the Nafion ionomer lowers the proton diffusion rate and contributes to an elevated local pH on the cathode,[10b] providing a suitable surface environment for BHMF production.[15] As controls, we coated anionic ionomers (PiperION and Sustainion) and found that these led to a diminution in BHMF FE (Figure 3B). The ionomer coating strategy was extended to other catalysts active in HMF electroreduction (Figure 3D). We observed similar trends when we used Ag and AgCu nanoparticles: the presence of a cationic ionomer layer on the catalyst surface improves ECH selectivity and FE toward BHMF at 100 mA cm^{-2} (Figure S4, Supporting Information).

We characterized operating stability at 100 mA cm^{-2}, finding that the ionomer-enhanced catalyst exhibited an average BHMF FE of 51% over the course of 8 h of continuous flow electrosynthesis (Figure 3E), with voltage always at or below 3.27 V full cell when coupled with anodic OER. The average BHMF production rate was ≈1 $mmol^{-1}$ cm^{-2} h^{-1} in stability tests. A portion of the electrolyte was periodically removed to analyze the product. The catholyte was replaced with fresh electrolyte after 6 h of ECH to maintain a constant HMF concentration during the stability test.

2.3. Mechanistic Studies

Building on previous studies of BHMF formation pathways,[6d,15] we investigated the catalytic mechanism. In linear sweep voltammetry (LSV) experiments without HMF (**Figure 4A** and Figure S5A, Supporting Information), the ionomer-coated

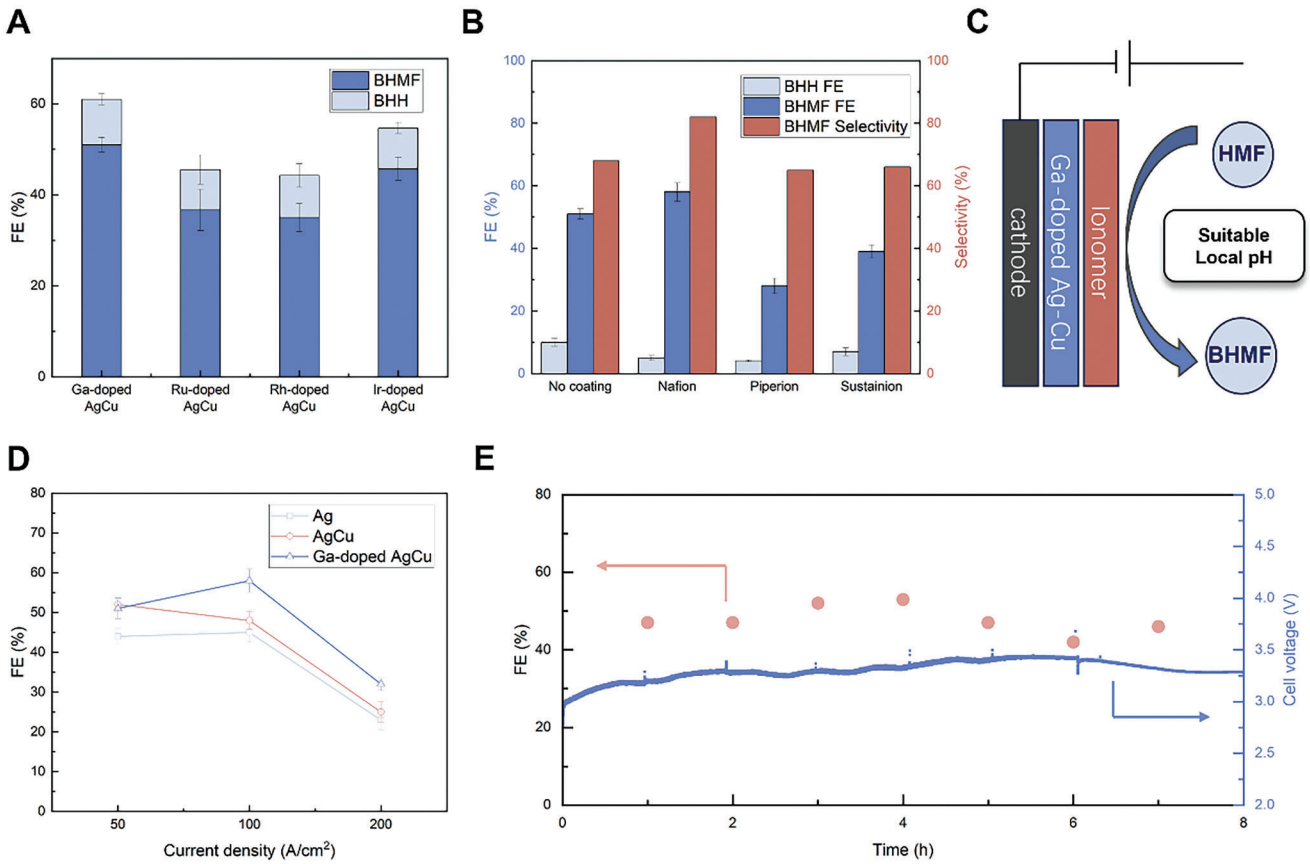

Figure 3. Evaluation of BHMF production. A) Doped catalysts for HMF electroreduction at 100 mA cm^{-2}. B) Selective electroreduction of HMF on different ionomer-coated Ga-doped Ag-Cu catalysts at 100 mA cm^{-2}. C) Surface modification of ECH catalyst. D) Electroreduction of HMF to BHMF at different current densities using ionomer-coated catalysts. E) BHMF FE and cell voltage during 8 h of HMF reduction at 100 mA cm^{-2} using the $Ga_1Cu_{21}Ag_{88}$ catalyst. Red: FE for BHMF; blue: Cell voltage.

Ga-doped Ag-Cu catalyst exhibited enhanced water reduction ability compared to other ECH-active catalysts and compared to uncoated catalysts, indicating a superior ability to generate surface adsorbed hydrogen atoms (H_{ads}) necessary for ECH. The addition of HMF into the electrolyte led to a reduction peak, which we link to HMF to BHMF, at −1.15 V versus Ag/AgCl (Figure 4B and Figure S5B, Supporting Information). We employed in situ Raman spectroscopy to study the effects of Ga doping (Figure S6, Supporting Information). On Ga-doped Ag-Cu (Figure S6A, Supporting Information), we observed the C = C stretching vibration of the furan ring at 1525 and 1560 cm^{-1}, indicating the adsorption of HMF near the catalyst surface.[16] The band at 1664 cm^{-1}, correlated to the C = O stretching in HMF,[17] appears at a potential of −1.1 V on Ga-doped Ag-Cu. The C = O stretching band was not found in control experiments on AgCu (Figure S6B, Supporting Information). These results suggest that Ga incorporation into AgCu enhances the binding of the carbonyl group of the HMF to the catalyst surface, promoting selectivity towards BHMF in electro-hydrogeneration.

Previous reports[6a,15,18] demonstrated that HMF reduction selectivity depends strongly dependence on electrolyte pH; with these studies finding that a suitably alkaline condition is needed to promote BHMF production. A similar trend of pH dependence in BHMF FE is observed using the AgCu catalyst in the high current density region (Figure S7, Supporting Information). We offer that the cationic ionomer layer enhances proton migration and provides alkaline local conditions at the cathode surface.[11] Additionally, the alkaline environment favors the hydrogen atom transfer (HAT) process,[15] which promotes kinetically the transfer of H_{ads} to organic species instead of undergoing the HER.

Based on the in situ Raman results, we offer that Ga doping promotes the adsorption of HMF on Ag-active sites. The incorporation of Ag with Cu serves to stabilize H_{ads}[19] and limits its competing HER in HMF electroreduction according to the LSV studies (Figure 4A). The cationic ionomer layer on the optimized catalyst tunes the cathodic environment to a suitable local pH, improving BHMF selectivity. We summarize in Figure 4C an HMF reduction catalytic cycle: HMF first interacts with the catalyst and forms an organic-adsorbed surface intermediate; the hydrogen addition step is accomplished either by the proton transfer from solution through proton-coupled electron transfer (PCET) or by direct addition of H_{ads} to the adsorbed intermediate through HAT. A limited supply of protons in alkaline conditions hinders direct PCET, a reaction that normally leads to HMF dimerization.[15] The H_{ads} produced from the Volmer step of HER[18] sets the stage for hydrogen addition to the aldehyde group. Finally, the desired BHMF is released via a HAT process.

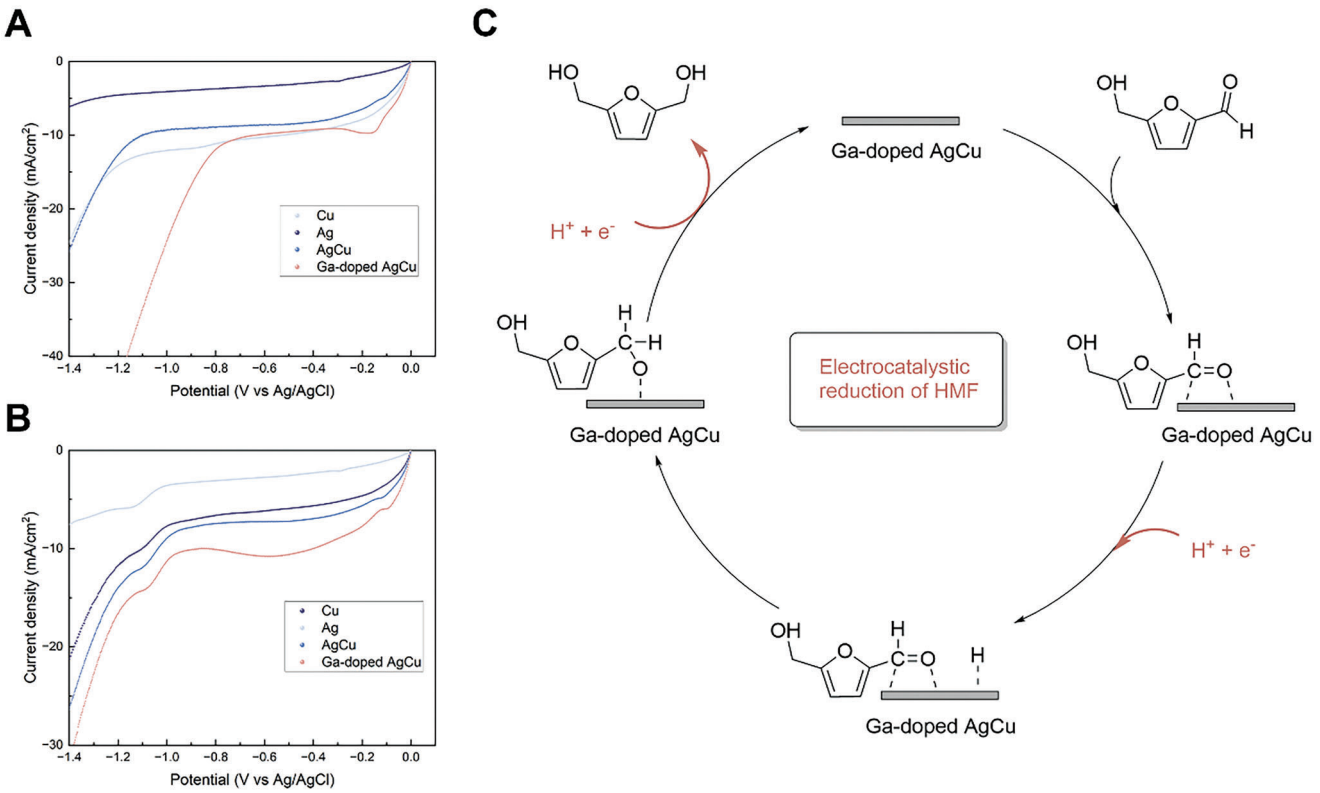

Figure 4. Proposed mechanism of electrocatalytic hydrogenation for BHMF production. Linear sweep voltammetry spectra for A) prepared catalysts in 1 M $NaHCO_3$ and B) 1 M $NaHCO_3$ and 0.01 M HMF at 10 mV s^{-1} without iR correction. C) Schematic of the proposed mechanism for BHMF production.

3. Conclusion

This work reports the electrosynthesis of BHMF using industrially relevant current densities. We synthesized Ga-doped Ag-Cu nanodendrites towards the goal of selective HMF ECH toward BHMF. By applying a hybrid strategy based on *p*-block Ga-doped materials combined with a cationic ionomer layer, we increased the local pH, suppressing competing HER and improving ECH selectivity. A BHMF FE of 58% and selectivity of 82% were achieved at 100 mA cm^{-2}. This strategy provided a BHMF productivity of 1 $mmol^{-1}$ cm^{-2} h^{-1} during continuous operation over an initial 8-h period of study. This work advances the electroreductive valorization of biomass potentially relevant to the production of biopolymer precursors under conditions of increased activity.

Supporting Information

Supporting Information is available from the Wiley Online Library or from the author.

Acknowledgements

C.T. and J.Y. contributed equally to this work. This work made use of the EPIC, Keck-II, and SPID facility of Northwestern University's NUANCE Center, which has received support from the ShyNE Resource (NSF ECCS-2025633), the IIN, and Northwestern's MRSEC program (NSF DMR-2308691). J.Y. thanks for the support from the International Institute for Nanotechnology.

Conflict of Interest

The authors declare no conflict of interest.

Data Availability Statement

The data that support the findings of this study are available from the corresponding author upon reasonable request.

Keywords

2,5-bis(hydroxymethyl)furan, biomass valorization, electrocatalytic reductions, nanodendrites

Received: November 27, 2023
Revised: February 26, 2024
Published online:

[1] S. A. Akhade, N. Singh, O. Y. Gutiérrez, J. Lopez-Ruiz, H. Wang, J. D. Holladay, Y. Liu, A. Karkamkar, R. S. Weber, A. B. Padmaperuma, M.-S. Lee, G. A. Whyatt, M. Elliott, J. E. Holladay, J. L. Male, J. A. Lercher, R. Rousseau, V.-A. Glezakou, *Chem. Rev.* **2020**, *120*, 11370.

[2] B. H. R. Suryanto, K. Matuszek, J. Choi, R. Y. Hodgetts, H.-L. Du, J. M. Bakker, C. S. M. Kang, P. V. Cherepanov, A. N. Simonov, D. R. MacFarlane, *Science*. **2021**, *372*, 1187.
[3] B. Zhang, B. K. Biswal, J. Zhang, R. Balasubramanian, *Chem. Rev.* **2023**, *123*, 7193.
[4] J. J. Bozell, G. R. Petersen, *Green Chem.* **2010**, *12*, 539.
[5] a) M. T. Bender, X. Yuan, M. K. Goetz, K.-S. Choi, *ACS Catal.* **2022**, *12*, 12349; b) Y. Gao, L. Ge, H. Xu, K. Davey, Y. Zheng, S.-Z. Qiao, *ACS Catal.* **2023**, *13*, 11204.
[6] a) G. S. de Luna, A. Sacco, S. Hernandez, F. Ospitali, S. Albonetti, G. Fornasari, P. Benito, *ChemSusChem*. **2022**, *15*, 202102504; b) G. Sanghez de Luna, P. H. Ho, A. Sacco, S. Hernández, J.-J. Velasco-Vélez, F. Ospitali, A. Paglianti, S. Albonetti, G. Fornasari, P. Benito, *ACS Appl. Mater. Interfaces*. **2021**, *13*, 23675; c) G. Sanghez de Luna, P. H. Ho, A. Lolli, F. Ospitali, S. Albonetti, G. Fornasari, P. Benito, *ChemElectroChem*. **2020**, *7*, 1238; d) J. J. Roylance, T. W. Kim, K.-S. Choi, *ACS Catal.* **2016**, *6*, 1840; e) Y. Kwon, E. de Jong, S. Raoufmoghaddam, M. T. M. Koper, *ChemSusChem*. **2013**, *6*, 1659.
[7] a) H. Zhou, Y. Ren, B. Yao, Z. Li, M. Xu, L. Ma, X. Kong, L. Zheng, M. Shao, H. Duan, *Nat. Commun.* **2023**, *14*, 5621; b) H. Liu, T.-H. Lee, Y. Chen, E. W. Cochran, W. Li, *ChemElectroChem*. **2021**, *8*, 2817; c) H. Liu, T.-H. Lee, Y. Chen, E. W. Cochran, W. Li, *Green Chem*. **2021**, *23*, 5056; d) K. Gu, D. Wang, C. Xie, T. Wang, G. Huang, Y. Liu, Y. Zou, L. Tao, S. Wang, *Angew. Chem., Int. Ed.* **2021**, *60*, 20253; e) Y. Lu, T. Liu, C.-L. Dong, Y.-C. Huang, Y. Li, J. Chen, Y. Zou, S. Wang, *Adv. Mater.* **2021**, *33*, 2007056.
[8] P. De Luna, C. Hahn, D. Higgins, S. A. Jaffer, T. F. Jaramillo, E. H. Sargent, *Science*. **2019**, *364*, aav3506.
[9] a) P. Li, J. Bi, J. Liu, Y. Wang, X. Kang, X. Sun, J. Zhang, Z. Liu, Q. Zhu, B. Han, *J. Am. Chem. Soc.* **2023**, *145*, 4675; b) Y. Wang, M. Zheng, Y. Li, C. Ye, J. Chen, J. Ye, Q. Zhang, J. Li, Z. Zhou, X.-Z. Fu, J. Wang, S.-G. Sun, D. Wang, *Angew. Chem., Int. Ed.* **2022**, *61*, 202115735.
[10] a) M. Fan, J. E. Huang, R. K. Miao, Y. Mao, P. Ou, F. Li, X.-Y. Li, Y. Cao, Z. Zhang, J. Zhang, Y. Yan, A. Ozden, W. Ni, Y. Wang, Y. Zhao, Z. Chen, B. Khatir, C. P. O'Brien, Y. Xu, Y. C. Xiao, G. I. N. Waterhouse, K. Golovin, Z. Wang, E. H. Sargent, D. Sinton, *Nat. Catal.* **2023**, *6*, 763; b) C. Kim, J. C. Bui, X. Luo, J. K. Cooper, A. Kusoglu, A. Z. Weber, A. T. Bell, *Nat. Energy*. **2021**, *6*, 1026.
[11] F. P. García de Arquer, C.-T. Dinh, A. Ozden, J. Wicks, C. McCallum, A. R. Kirmani, D.-H. Nam, C. Gabardo, A. Seifitokaldani, X. Wang, Y. C. Li, F. Li, J. Edwards, L. J. Richter, S. J. Thorpe, D. Sinton, E. H. Sargent, *Science*. **2020**, *367*, 661.
[12] Y. Zhong, R. Ren, Y. Peng, J. Wang, X. Ren, Q. Li, Y. Fan, *Mol. Catal.* **2022**, *528*, 112487.
[13] R. Kloth, D. V. Vasilyev, K. J. J. Mayrhofer, I. Katsounaros, *ChemSusChem*. **2021**, *14*, 5245.
[14] R. Dorakhan, I. Grigioni, B.-H. Lee, P. Ou, J. Abed, C. O'Brien, A. Sedighian Rasouli, M. Plodinec, R. K. Miao, E. Shirzadi, J. Wicks, S. Park, G. Lee, J. Zhang, D. Sinton, E. H. Sargent, *Nat. Synth.* **2023**, *2*, 448.
[15] X. Yuan, K. Lee, M. T. Bender, J. R. Schmidt, K.-S. Choi, *ChemSusChem*. **2022**, *15*, 202200952.
[16] N. Heidary, N. Kornienko, *Chem. Commun.* **2019**, *55*, 11996.
[17] N. Heidary, N. Kornienko, *Chem. Sci.* **2020**, *11*, 1798.
[18] K. Ji, M. Xu, S.-M. Xu, Y. Wang, R. Ge, X. Hu, X. Sun, H. Duan, *Angew. Chem., Int. Ed.* **2022**, *61*, 202209849.
[19] J. Greeley, T. F. Jaramillo, J. Bonde, I. Chorkendorff, J. K. Nørskov, *Nat. Mater.* **2006**, *5*, 909.